Austin Journal of Pharmacology and Therapeutics

Open Access

Austin Publishing Group

Research Article

Suplatast Tosilate Inhibited Nicotinic Single-Channel Currents in the Paratracheal Ganglia Neurons of Rats

Jian-Rong Zhou[1,2], Tetsuya Shirasaki[1,3], Fumio Soeda[1,4] and Kazuo Takahama[1]*

[1]Department of Environmental and Molecular Health Sciences, Kumamoto University, Japan

[2]Department of Presymptomatic Medical Pharmacology, Sojo University, Japan

[3]Department of Environmental and Health Sciences, Kyushu University of Health and Welfare, Japan

[4]Laboratory of Hygienic Chemistry, Daiichi University of Pharmacy, Japan

***Corresponding author:** Kazuo Takahama, Department of Environmental and Molecular Health Sciences, Kumamoto University, Japan

Received: December 01, 2020; **Accepted:** December 24, 2020; **Published:** December 31, 2020

Abstract

Suplatast tosilate, an antiallergic agent, is effective for cough variant asthma, although the definitive mechanism is not clear. We have reported that suplatast inhibition of nicotinic current in paratracheal ganglia neurons is noncompetitive, voltage-dependent and use-independent, suggesting probably *via* an open channel block. In this study, we investigated the effects of suplatast on nicotine-induced single-channel current in neurons dissociated from rat paratracheal ganglia using outside-out patch-clamp recording. The data showed that suplatast induced very brief duration currents of nicotinic receptor/channels and should be expected open channel flickering, thus suplatast works as a nicotinic open channel blocker. These results suggest that suplatast might inhibit neurotransmission at the paratracheal ganglia *via* the inhibition of nicotinic current. Consequently, the drug may improve pathological conditions of the lower airway, leading to an increased threshold of cough production.

Keywords: Suplatast; Nicotinic Acetylcholine Receptor; Paratracheal Ganglion Neuron; Outside-Out Mode Patch-Clamp Recording

Introduction

Suplatast (suplatast tosilate, ((±)-[2-[4-(3-ethoxy-2-hydroxy-propoxy) phenylcarbamoyl] ethyl] dimethylsulfonium p-toluenesulfonate)) is a selective Th2 cytokine inhibitor [1]. We found that suplatast inhibited the codeine-resistant coughs in bronchitis model of guinea pigs prepared by exposure to SO_2 gas and the citric acid-induced coughs in guinea pigs pretreated with an angiotensin-converting enzyme inhibitor [2]. Also, in clinic, it has been reported that suplatast improved the cough score and the cough threshold for capsaicin in patients with cough variant asthma [3]. Moreover, suplatast has been reported to be effective in treating coughs persisting for more than two weeks [4], chronic cough, atopic cough and allergic eosinophilic airway inflammation [5-7]. Thus, suplatast has an antitussive effect on cough variant asthma in human and codeine-resistant cough in animal models. However, the antitussive effect of suplatast does not appear to be due to the anti-allergic effect caused by Th2 cytokine inhibition [8]. The predominant control of airways is exerted by cholinergic nerves. Cholinergic nerves in the airways arise from the paratracheal ganglia, which situate on the serosal surface of the dorsal tracheal wall. Short postganglionic fibers from paratracheal ganglia innervate airway smooth muscle, blood vessels, and submucosal glands. Cholinergic nerves also activate the mast cells [9,10]. In addition to central regulation by vagal preganglionic nerve fibers, paratracheal ganglia neuron excitability can be modulated by a peripheral C-fiber reflex mechanism [11-13]. The C-fiber terminals not only generate electric signals that conduct to the central nervous system but also cause antidromic release of neurokinins from the C-fiber terminal *via* an axon reflex [14]. Endogenous neurokinins facilitate the synaptic transmission in the airway parasympathetic ganglia [15]. We also found that bradykinin, a potent inflammatory peptide induced action-potential generation, potentiated the nicotinic current and cholinergic Excitatory Postsynaptic Currents (EPSCs) in acutely dissociated paratracheal ganglia neurons [16-18]. Therefore, the paratracheal ganglia may serve as critical sites for the pathogenesis of airway inflammation associated with cough. We previously found the presence of a voltage-dependent block of macroscopic nicotinic currents by suplatast tosilate demonstrates the existence of an open-channel blockade. Moreover, the presence of hump currents at high nicotine concentrations [8] also supports this mechanism of action. In the present study, we tried to record the nicotinic single-channel in paratracheal ganglia of rats and the effect by suplatast. Our results show that suplatast inhibits the nicotinic single-channel current in airway parasympathetic neurons *via* a rapid transient block of the open channel.

Materials and Methods

Dissociation of paratracheal ganglia neurons

The paratracheal ganglia neurons were dissociated from 12 day to 18-day old Wistar rats. The dissociation technique is described elsewhere [16]. Briefly, the paratracheal ganglia was rapidly removed with the trachea from animals under pentobarbital anesthesia, and were detached from the trachea under stereomicroscope, followed by treatment with 0.3% collagenase and 0.3% trypsin for 60 min at 34°C. The paratracheal ganglia neurons were then mechanically dissociated with a fine glass pipette by gently triturating the ganglia under an inverted phase-contrast microscope.

Electrophysiological recordings

Electrical measurements were performed by using the outside-out mode patch-clamp recording [19,20]. The patch electrode resistance was 5 to 8 MΩ.

Current and voltage signals were recorded with an Axopatch-200B patch-clamp amplifier (Molecular Devices, Union city, CA, U.S.A.) and acquired with pCLAMP7 data acquisition software (Molecular

Citation: Zhou J-R, Shirasaki T, Soeda F and Takahama K. Suplatast Tosilate Inhibited Nicotinic Single-Channel Currents in the Paratracheal Ganglia Neurons of Rats. Austin J Pharmacol Ther. 2020; 8(2).1125.

Devices) after digitization with a Digidata 1200B (Molecular Devices). All experiments were performed at room temperature (21˚C to 24˚C). Recordings were conducted using neurons with resting membrane potentials of -55 mV to -80 mV. For single-channel recording, patch currents were digitized at 100 kHz and filtered at a cutoff frequency (f_1) of 5 kHz using the Bessel filter and then at 16.7 kHz (f_2) during data analysis. To accurately resolve the events, we used the criterion that only events above a preset amplitude having durations more than two times the rise time (tr=0.3321/*fc*) of the Bessel filter would be accepted for analysis [21,22].

Single channel events were detected by visual inspection of the transitions from the base current and manually selected using Fetchan software of pCLAMP 7.0. Thereafter, events were compiled into all-points histograms using 0.6 ms bin width and were fitted with Gaussian functions using a simplex least-squares algorithm in pSTAT of pCLAMP 7.0. The frequency of opening for each event was determined by the reciprocal of the open + closed time since the last event. To gain more information about steady-state open probabilities, we assumed nicotinic acetylcholine channels obey a modified Castillo and Katz activation scheme [21] such that channels can exist in n +1 closed states (R, A_1R, A_2R ...A_nR), but only 1 open state (A_nR^*). The probability of a channel being open (NPo) was measured over specific time intervals, thus providing a quantitative description of the activity of the channel *vs.* time. For determination of mean open and closed time, open and closed duration was respectively compiled in conventional and logarithmic histograms and then fitted by simplex least square method for open time and maximum likelihood method for closed time.

Solution and chemicals

The ionic composition of the Krebs solution was (in mM): NaCl 121.7, KCl 4.7, $MgCl_2$ 1.2, $CaCl_2$ 2.5, glucose 11.5, $NaHCO_3$ 15.5 and KH_2PO_4 1.2. The solution was carbonated with 95% O_2 and 5% CO_2. The ionic composition of the normal external solution was (in mM): NaCl 131.7, KCl 5, $MgCl_2$ 1.2, $CaCl_2$ 2.5, HEPES 10 and glucose 11.5. The pH was adjusted to 7.4 with NaOH. The composition of the pipette solution for the single-channel recording was (in mM): NaCl 20, KCl 50, K-gluconate 70, $MgCl_2$ 3, $CaCl_2$ 0.246, HEPES 10, EGTA 5 and ATP-2Na 2. The pH was adjusted to 7.2 with 1N KOH. A rapid application of external solution was performed using the 'Y-tube' technique described previously [22]. With this technique, the external solution was completely exchanged within 30 ms.

Collagenase, nicotine, and trypsin were purchased from Sigma (St. Louis, MO, USA). Suplatast tosilate was synthesized and supplied by Taiho Pharmaceutical Co. Ltd. (Tokyo, Japan).

Statistical analysis

Each value represents the mean ± SE for at least 5 cells. Comparisons between the two groups were carried out by paired or unpaired Student's t-test. Multiple comparisons were performed by Dunnett's test. Probability (P) values less than 0.05 were considered to be statistically significant.

Results

Property of nicotine-induced single-channel current

For single-channel analysis of nicotinic response, we first used a concentration of 10M to 5 M of nicotine close to the EC50 for nicotinic response (Figure 1A). However, this concentration of nicotine was inappropriate for the single-channel analysis, because this concentration activated multiple nicotinic acetylcholine receptor/channel complexes simultaneously in outside-out mode of patch clamp. Therefore, $3x10^{-6}$ M nicotine was used for single channel analysis in outside-out mode. As shown in Figure 1B, single-channel current (i_{Nic}) amplitude became larger at lower holding potentials (Figure 1). In Figure 2A-C, all-points amplitude histograms at each potential were prepared by using the bin width of 0.6 ms (256 bins), which provides the finest resolution. The distributions were well

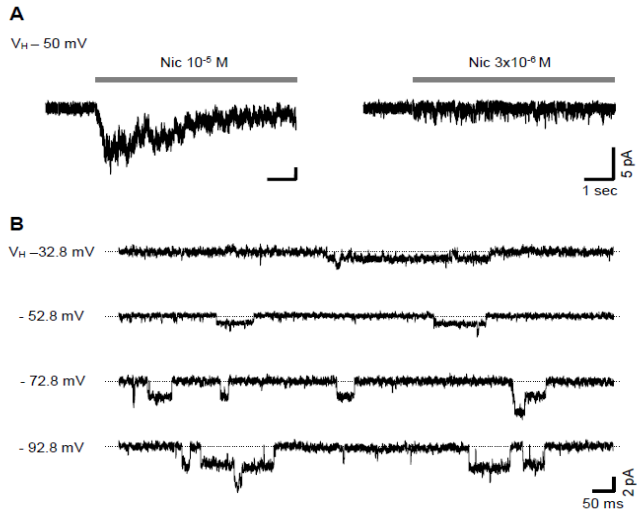

Figure 1: Single nicotinic channel currents recorded by using outside-out mode of patch clamp in rat PTG neuron. A: single-channel currents induced by 10^{-5} M and 3×10^{-6} M nicotine at a V_H of -50 mV. Bars indicate the period of nicotine application. B: expanded traces showing 3×10^{-6} M nicotine-induced single-channel currents (i_{Nic}) at different holding potentials. Dashed lines represent closed.

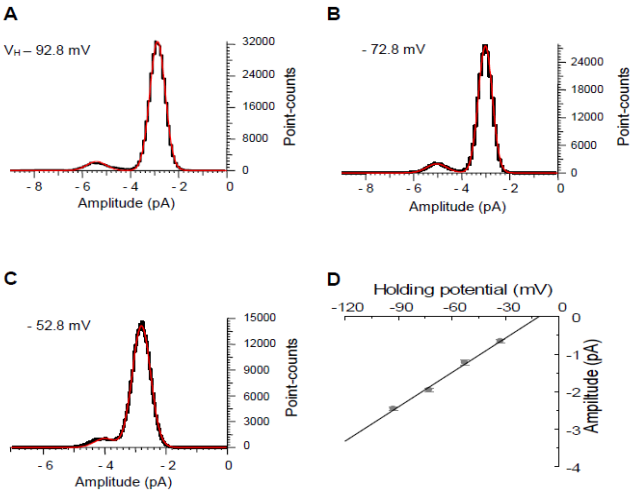

Figure 2: Single-channel conductance for nicotine in PTG neurons. A. B. C: representative all point current amplitude histograms in the presence of 3×10^{-6} M nicotine at different holding potentials (black lines). The histograms were well fitted with 2 Gaussian functions (red curves). D: single channel current-voltage relationship for nicotine. Single channel current amplitudes calculated from the all points current amplitude histograms were plotted against the holding potentials.

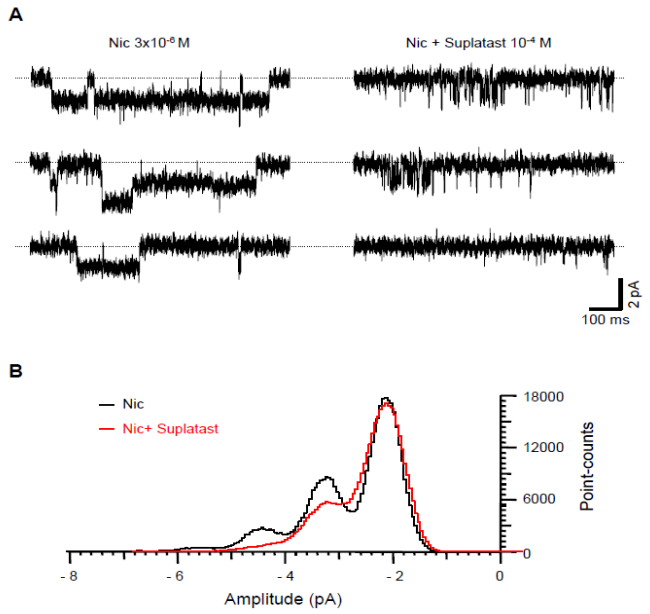

Figure 3: Effects of suplatast on nicotinic single channel current. A: representative record showing 3×10^{-6} M nicotine-induced single-channel currents in the absence and presence of 10^{-4} M suplatast at a V_H of –50 mV. Note that suplatast caused flickering of channel open in right traces. B: representative all point current amplitude histograms showing the effect of suplatast. Note that suplatast reduced the height of second to fourth peaks but did not change the position of peaks in Gaussian distribution.

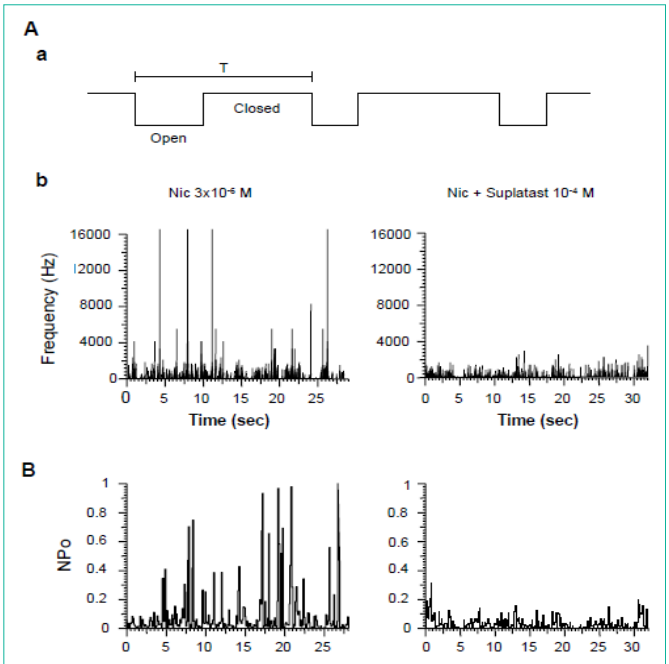

Figure 4: Effect of suplatast on channel opening frequency and the open probability of nicotinic channel in PTG neuron. A: determination of channel opening frequency. a: the frequency (f) of opening for each event is determined by the reciprocal of the open + closed time (T) since the last event. b: changes in nicotinic channel opening frequency along the time a× is in the absence and presence of 10^{-4} M suplatast. B: changes in open probability (NPo) of nicotinic channel along the time axis in the absence and presence of 10^{-4} M suplatast. In this patch, NPo was reduced from 0.092±0.17 (n=3740) to 0.035±0.22 (n=3240).

fitted with two or three Gaussian functions. To better illustrate the main channel conductance, single channel current amplitude at each potential was determined as the difference between the current amplitudes of two peaks laying side-by-side. In Figure 2D, the mean single channel current amplitude at each potential was plotted against the holding potential. The result was fitted with the linear function and the conductance of 23.7 pS was obtained from the slope of straight line which reversed at around -10 mV (Table 1) (Figure 2).

Effect of suplatast on nicotinic single-channel

When membrane patch was pretreated with 10^{-4} M suplatast for 30 s and then nicotine and suplatast was simultaneously applied, the open duration of the channel was obviously shortened and the flickering of channel open was observed (Figure 3A). Suplatast should be expected open channel flickering resulting in very brief duration currents without affecting the unitary current amplitude in the amplitude histogram (Figure 3B). Nicotinic single-channel conductance was 23.2±0.47 pS in the presence of suplatast (Table 1) (Figure3).

The frequency of channel open and the open probability (NPo) were also reduced by suplatast (Figure 4A and 4B). NPo in control conditions oscillated between 0 and 1 in multiple levels (Nicotine 3x10^{-6} M). In presence of suplatast, NPo remained close to 0.1, showed a transient block on open channel. The open probability of nicotinic single-channel was shown as 0.13±0.06, and was reduced to 0.09±0.03 with 10^{-4} M suplatast (Table 1) (Figure 4).

To investigate the open and close kinetics of nicotinic acetylcholine receptor/channel complex, open and closed durations were analyzed in patches in which the total numbers of events exceeded 1000. Open duration was compiled in conventional histograms and fitted by simplex least square method using the bin width of 0.06 ms (Figure 5A). The bin width was selected as an integer multiple of the sampling rate (0.06 ms) to scale a linear histogram and correct the binning and sampling promotion errors. The distribution of open duration for nicotine was well characterized by two open time constants, τ_{O1} 1.29±0.07 ms and τ_{O2} 3.13±0.47 ms, or by two open proportions, 78.6±5.86 % and 21.4±5.86 %. Suplatast significantly shortened these two open time constants as 0.77±0.16 ms and 1.02±0.02 ms, and their two open proportions were shown as 66.2±16.42 % and 45.07±16.89 %, respectively (Table 1). Since the closed duration was distributed in a wide range of 0.3 ms to 58 ms, it was compiled in logarithmic histograms and fitted by maximum likelihood method using the bin width of 0.06 ms (Figure 5B). In maximum likelihood method, data may be binned into the variable width in a logarithmic histogram. The distribution of closed duration for nicotine was well characterized by two closed time constants, τ_{C1} 1.31±0.13 ms and τ_{C2} 10.81±1.09 ms, or by two close proportions, 34.28±2.27 % and 65.72±2.27 %. Suplatast prolonged these two closed time constants as 2.0±0.27 ms and 17.27±2.02 ms, respectively, and their two close proportions were shown as 52.02±5.6 % and 47.9±5.6 %, respectively (Table 1) (Figure 5).

Since the flickering of channel open was observed in the presence of suplatast, burst analysis was further performed. Bursts were defined as groups of openings separated by interburst interval. Interburst interval, i.e., the minimum value of a closed duration

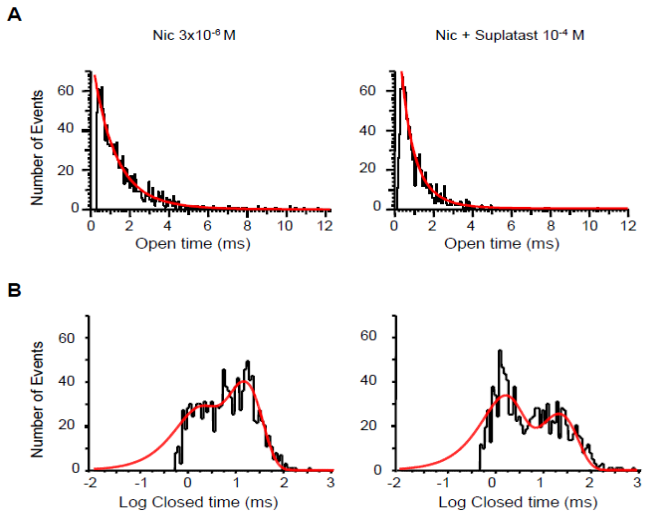

Figure 5: Effects of suplatast on open and closed time of nicotinic channel. A: distributions of single-channel open time in the absence and presence of 10^{-4} M suplatast. Each distribution was fitted with two exponential functions. Estimated open time constants τ_{O1} and τ_{O2} for 3×10^{-6} M nicotine were 1.29 ms and 3.13 ms and their proportions were 79 % and 21 %, respectively. In the presence of suplatast, these became 0.77 ms (66 %) and 1.02 ms (45 %), respectively. B: distributions of single-channel closed time in common logarithmic scale in the absence and presence of 10^{-4} M suplatast. Each distribution was fitted with two Gaussian functions. Estimated closed time constants τ_{C1} and τ_{C2} (and their proportion) were 1.31 ms (34 %) and 10.8 ms (66 %), respectively. In the presence of suplatast, these became 2.0 ms (52 %) and 17.27 ms (48 %), respectively.

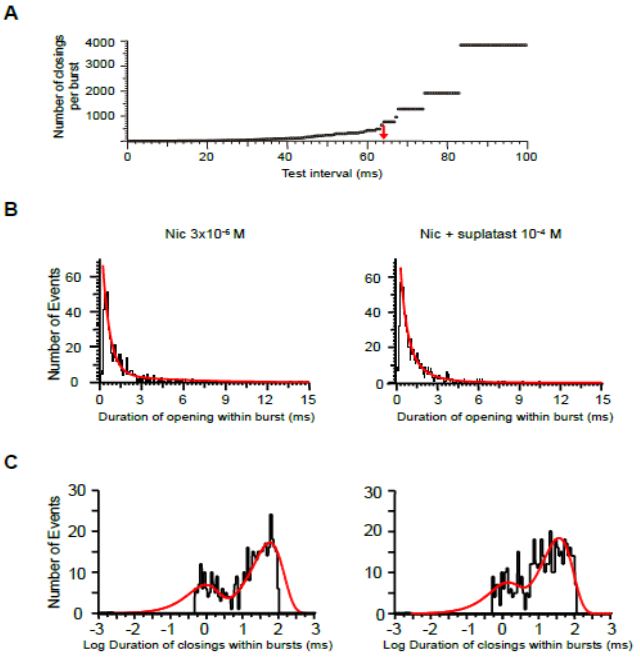

Figure 6: Effects of suplatast on burst of nicotinic channel. A: representative analysis for determining the proper interburst interval. The point indicated by arrow is the optimal interburst interval. B: distributions of open time during burst in the absence and presence of 10^{-4} M suplatast. Each distribution was fitted by two exponential functions. Estimated open time constants τ_{BO1} and τ_{BO2} (and their proportion) in burst for 3×10^{-6} M nicotine were 0.55 ms (75 %) and 4.52 ms (25 %), respectively. In the presence of suplatast, these became 0.75 ms (50 %) and 1.87 ms (50 %), respectively. C: distributions of closed time during burst in common logarithmic scale in the absence and presence of 10^{-4} M suplatast. Each distribution was fitted by two Gaussian functions. Estimated closed time constants in burst τ_{BC1} and τ_{BC2} (and their proportion) for nicotine 3×10^{-6} M were 0.67 ms (33 %) and 41.7 ms (67 %), respectively. In the presence of suplatast, these became 1.21 ms (42 %) and 16.54 ms (68 %), respectively.

which separates the burst was determined as shown in Fig.6A. When the test interburst interval becomes identical to the 'true' interburst interval, and if the bursts are reasonably well-delineated, the number of closings per "burst" will be relatively insensitive to further changes in the test interburst interval [23]. This point is the optimal interburst interval. In the case of Figure 6A, this value was 64 ms.

Suplatast significantly reduced the open probability within bursts from 0.74±0.04 to 0.54±0.04 (Table 1). Open duration in burst was compiled in conventional histograms and fitted by simplex least square method using the bin width of 0.06 ms (Figure 6B). The distribution for nicotine of open duration in burst was well characterized by two open time constants, τ_{BO1} 0.55±0.09 ms and τ_{BO2} 4.52±1.03 ms. Suplatast prolonged τ_{BO1} as 0.75±0.24 ms, but significantly shortened τ_{BO2} as 1.87±0.25 ms (Table 1). On the other hand, closed duration in burst was compiled in logarithmic histograms and fitted by maximum likelihood method using the bin width of 0.06 ms (Figure 6C). The distribution for nicotine of closed duration in burst was well characterized by two closed time constants τ_{BC1} 0.67±0.08 ms and τ_{BC2} 41.71±5.7 ms. Suplatast prolonged τ_{BC1} as 1.21±0.31 ms, but significantly shortened τ_{BC2} as 16.54±3.64 ms (Table 1) (Figure 6).

Discussion

We revealed in this study that suplatast inhibited nicotine-induced single-channel current in rat paratracheal ganglia neurons. Furthermore, the present study showed that in outside-out mode of patch clamp, suplatast induced very brief duration of nicotinic receptor/channels and should be expected open channel flickering. These suggest that the inhibition of suplatast may be the open channel block.

Firstly, we investigated the property of single i_{Nic} in rat parasympathetic paratracheal ganglia neurons. The i_{Nic} amplitude followed Ohm's law at negative membrane potentials but tended to reach a plateau at positive membrane potentials (Figure1). The mean slope conductance measured between -90 and -30 mV was 23.7 pS (Figure 2 and Table 1). And the number of functional channels and the probability of a channel being open showed a voltage dependence. Similar small conductance has been observed in rat cardiac neurons (26 pS) and mouse submandibular ganglion cells (28.5 pS) [24-26] in contrast to the primary conductance of rat sympathetic SCG neurons 34.8 pS - 36.6 pS [27]. It has been reported that airway parasympathetic neurons express nicotinic acetylcholine receptors containing $\alpha3\beta4$ subunits based on immunohistochemical staining by Weigand [28], and this subtype can form pentameric receptors with either 2 or 3 $\beta4$ subunits [29]. Furthermore, distinct stoichiometric isoforms (manipulations of the $\alpha3$:$\beta4$ subunit ratios) of $\alpha3\beta4^{*}$ nicotinic acetylcholine receptors expressed in oocytes differed in their single-channel properties, for example, the three α isoform had a larger single-channel conductance [30,31]. Thus, these suggest that two $\alpha3$ and three $\beta4$ subunits may be the main isoforms of nicotinic

Table 1: Effects of suplatast on single channel properties. Data were presented as mean ± S.E.M.

	Nicotine 3×10^{-6} M	Nicotine+ Suplatast 10^{-4} M
Conductance (pS)	23.7±0.74	23.7±0.47
Open probability	0.13±0.06	0.09±0.03
Open time [ms (%)]		
τ_{O1} (Proportion)	1.29±0.07 (78.6±5.86)	0.77±0.16* (66.20±16.42)
τ_{O2} (Proportion)	3.13±0.47 (21.4±5.86)	1.02±0.02* (45.07±16.89)
Closed time [ms (%)]		
τ_{C1} (Proportion)	1.13±0.13 (34.28±2.27)	2.0±0.27 (52.02±5.60)
τ_{C2} (Proportion)	10.81±1.09 (65.72±2.27)	17.27±2.02* (47.9±5.60)
Open probability within bursts	0.74±0.04	0.54±0.04*
Opening duration within bursts [ms (%)]		
τ_{BO1} (Proportion)	0.55±0.09 (74.95±7.58)	0.75±0.24 (49.72±11.76)
τ_{BO2} (Proportion)	4.52±1.03 (25.05±7.58)	1.87±0.25* (50.28±11.76)
Closing duration within bursts [ms (%)]		
τ_{BC1} (Proportion)	0.67±0.08 (32.98±5.76)	1.21±0.31 (31.70±2.21)
τ_{BC2} (Proportion)	41.71±5.70 (67.02±5.76)	16.54±3.64* (68.3±2.21)

acetylcholine receptors expressed in rat paratracheal ganglia neurons, although, this remains to be studied.

In rat paratracheal ganglia neurons, nicotine-activated single-channel currents had two distinct open states with open times of 1.29 and 3.13 ms (referred to as primary $\tau_{O1}$and secondary τ_{O2}) at -50 mV in 131.7 mM of external Na^+ concentration and 20 mM of internal Na^+ concentration in the patch pipette. This primary τ_{O1} is consistent with the report that acetylcholine-activated single channel currents had an apparent mean open time of 1.15 ms at -60 mV in rat parasympathetic neurons [25]. Within burst, single i_{Nic} had two opening durations with open times of primary τ_{BO1} 0.55 ms and secondary τ_{BO2} 4.52 ms. In the presence of 10^{-4} M suplatast total primary and secondary open times (without and within burst) were both significantly reduced to 0.77 and 1.02 ms, respectively (Figure 3-5) without affecting the single-channel conductance (Table 1; slope conductance 23.2 pS *versus* 23.7 pS). Within burst of single i_{Nic}, suplatast significantly reduced secondary opening duration τ_{BO2} to 1.87 ms with reduced open probability of single-channel (Figure 6 and Table 1; 0.54 *versus* 0.74).

Further, single i_{Nic} had two distinct closed states. Suplatast markedly prolonged the primary closed time τ_{C2} from 10.81 ms to 17.27 ms (Figure 3-5). Within burst, suplatast markedly reduced secondary closed duration τ_{BC2} from 41.71 ms to 16.54 ms (Figure 6 and Table 1).

In general, these data suggest that at rat paratracheal ganglia neurons suplatast, pretreated for 30 s, inhibits single i_{Nic} *via* a rapid transient block of the open channel, decreasing the nicotinic acetylcholine receptor/channel open probability. This finding is also supported by our previous report that in whole-cell patch clamp, inhibition of I_{Nic} by suplatast was in voltage-dependent and noncompetitive manners since the effect of suplatast did not depend on the pretreatment time (from 10 s to 60 s) and suplatast inhibited the maximum I_{Nic}. In addition, the hump current was also observed after wash out of a higher concentration of nicotine in the presence of suplatast [8]. Thus, those voltage sensitivities recorded in whole-cell and outside-out patch clamp suggest that suplatast might bind at a site within the electric field, and those rapid transient blocks suggest that the target of suplatast might include the inner pore surface of the pore-forming region, of nicotinic acetylcholine receptor-channels in paratracheal ganglion neurons. Next, we should study voltage-dependence of single channel currents in presence of the molecule responsible of nicotinic inhibition.

Slightly higher concentrations were necessary to inhibit nicotinic current. As discussed in our previous study [8], however, a high dose such as 300 mg/day is treated for treating chronic cough in clinic. Consequently, plasma concentration (50 ng/ml) is also higher than other medicines (for example 50 μg/day and 100 pg/ml in the case of procaterol). In addition, suplatast at 10^{-4} M decreases the IL-4 production by 50% in D10G4.1 cell, a Th2 clone [32]. Mimura also indicated that suplatast inhibited the production of cytokines including IL-4 and IL-5 with IC50s of more than 10^{-4} M in both mouse splenocytes and human peripheral blood mononuclear cells [33]. Therefore, the concentrations required to inhibit nicotinic single-channel current are considered to be acceptable.

Suplatast tosilate is a novel dimethylsulphonium anti-allergic drug, protonated at pH equal to 7.4 (due to its pKa), but it is composed, additionally, by a p-toluenesulfonate (pKa = -2.14), which has a negative charge at pH 7.4. However, the basic salt, p-toluenesulphonic acid monohydrate at 50 ng/mL did not increase or decrease the chloride current in human blood eosinophils [34]. Next, we will investigate the effect of p-toluenesulphonic acid monohydrate on single paratracheal ganglia neurons.

Suplatast has an antitussive effect on cough variant asthma in humans and codeine-resistant cough in animal models. In clinics, bronchodilators have been recommended to treat the cough variant asthma, one of intractable cough. Hexamethonium, a ganglionic blocker, abolishes vagally-mediated bronchoconstriction [35]. In addition, hexamethonium inhibited allergic cough [36]. Therefore,

such a reduction of nicotinic acetylcholine receptor-channel activity by suplatast at paratracheal ganglia neuron might contribute to the antitussive effect of suplatast at least in patients with cough variant asthma [3]. Cough reflex is triggered by the stimulation of peripheral sensory nerve terminals and regulated by central and peripheral nervous system. Firstly, in sensory neurons, we have reported that suplatast may have no direct effect on the sensory nociceptive neurons/fibers [8]. Recently, we also found that histamine directly potentiated capsaicin-induced currents in rat sensory neurons, and suplatast had little effect on this potentiation [37]. Since suplatast is known to inhibit histamine releases from the mast cells [38], it is likely that suplatast indirectly inhibits sensitization of TRPV1 channel in nociceptive fibers and coughing *via* reduction of histamine release-induced pathological conditions. Secondly, in airway parasympathetic neurons, we found that in contrast to no effect on the bradykinin and muscarinic responses, suplatast directly depressed the excitability of paratracheal ganglia neuron *via* a block of nicotinic acetylcholine receptor/channel [8], which may be responsible for the attenuation of Excitatory Postsynaptic Potentials (EPSPs) at airway cholinergic synapses. Further studies are necessary to investigate the effect of suplatast on EPSP at the paratracheal ganglia.

In conclusion, suplatast inhibits nicotinic single channel current *via* an open channel block in paratracheal ganglia neurons, suggesting an inhibition of neurotransmission at the paratracheal ganglia and then an improvement of pathological conditions of the lower airway.

Acknowledgment

We wish to thank Taiho Pharmaceutical Co. Ltd., Japan, for donating the suplatast tosilate.

Statement of Ethics

All experiments were conducted in strict accordance with the Guideline of the Japanese Pharmacological Society for the Care and Use of Laboratory Animals. Animals were treated in accordance with Guide for the Care and Use of Laboratory Animals (8th edition, National Academies Press).

Author Contributions

J-R Zhou carried out patch clamp recording, and draft the manuscript. T Shirashaki and K. Takahama conceived of the study, participated in its design and drafted the manuscript. F. Soeda performed the statistical analysis. All authors read and approved the final manuscript.

References

1. Koda A, Yanagihara Y, Matsuura N. IPD-1151T: a prototype drug of IgE antibody synthesis modulation. Agents and actions Suppl. 1991; 34: 369-378.
2. Zhou J-R, Syono R, Fukumi S, Kimoto K, Shirasaki T, Soeda F, et al. Novel antitussive effect of suplatast tosilate in guinea pigs. Pharmacol. 2015; 95: 36-41.
3. Shioya T, Satake M, Sano M, Kagawa M, Watanabe A, Sato K, et al. Effect of suplatast tosilate, a Th2 cytokine inhibitor, on cough variant asthma. Eur J Clin Pharmacol. 2002; 58: 171-176.
4. Oota K. Marked antitussive effect of suplatast tosilate on persistent cough. Allergol & Immunol. 2003; 10: 67-72.
5. Miyamoto H, Sakao Y, Sakuraba M, Oh S, Takahashi N, Miyasaka Y, et al. Usefulness of suplatast tosilate for chronic cough following lung cancer surgery. Gen Thorac Cardiovasc Surg. 2009; 57: 463-466.
6. Ishiura Y, Fujimura M, Yamamoto H, Nobata K, Ishiguro T, Ogawa H, et al. Effect of an orally active Th2 cytokine inhibitor, suplatast tosilate on "atopic cough". Arzneimittelforschung. 2008; 58: 297-302.
7. Sano Y, Suzuki N, Yamada H, To Y, Ogawa C, Ohta K, Adachi M. Effects of suplatast tosilate on allergic eosinophilic airway inflammation in patients with mild asthma. J Allergy Clin Immunol. 2003; 111: 958-66.
8. Zhou J-R, Shirasaki T, Soeda F, Takahama K. The effects of suplatast tosilate on acutely dissociated sensory and paratracheal ganglia neurons. Am J Physiol Lung Cell Mol Physiol. 2016; 311: L770-778.
9. Reinheimer T, Baumgärtner D, Möhlig T, Racké K, Wessler I. Acetylcholine *via* muscarinic receptors inhibits histamine release from human isolated bronchi. Am J Respir Crit Care Med. 1997; 156: 389-95.
10. Schmelz M, Zeck S, Raithel M, Rukwied R. Mast cell tryptase in dermal neurogenic inflammation. Clin Exp Allergy. 1999; 29: 695-702.
11. Day RD, Altemus JB, Road A, Meyer B, Said SI, Coburn RF. Neurochemical characterization of intrinsic neurons in ferret tracheal plexus. Am J Respir Cell Mol Biol. 1996; 14: 207-216.
12. Myers AC, Undem BJ. Electrophysiological effects of tachykinins and capsaicin on guinea-pig bronchial parasympathetic ganglion neurones. J Physiol. 1993; 470: 665-679.
13. Myers AC, Undem BJ, Kummer W. Anatomical and electrophysiological comparison of sensory innervation of bronchial and tracheal parasympathetic ganglion neurons. J Auton Nerv Syst. 1996; 61: 162-168.
14. Barnes PJ. Asthma as an axon reflex. Lancet. 1986; 1: 242-245.
15. Canning BJ, Reynolds SM, Anukwu LU, Kajekar R, Myers AC: Endogenous neurokinins facilitate synaptic transmission in guinea pig airway parasympathetic ganglia. Am J Physiol Regul Integr Comp Physiol. 2002; 283: 320-330.
16. Mochidome T, Ishibashi H, Takahama K. Bradykinin activates airway parasympathetic ganglion neurons by inhibiting M-currents. Neurosci. 2001; 105: 785-791.
17. Zhou J-R, Shirasaki T, Soeda F, Takahama K. Potentiation of nicotinic currents by bradykinin in the paratracheal ganglia neurons of rats. Eur J Pharmacol. 2006; 531: 96-102.
18. Zhou JR, Shirasaki T, Soeda F, Takahama K. Cholinergic EPSCs and their potentiation by bradykinin in single paratracheal ganglion neurons attached with presynaptic boutons. J Neurophysiol. 2014; 112: 933-941.
19. Akaike N, Harata N. Nystatin perforated patch recording and its applications to analyses of intracellular mechanisms. Jpn J Physiol. 1994; 44: 433-473.
20. Horn R, Marty A. Muscarinic activation of ionic currents measured by a new whole-cell recording method. J Gen Physiol. 1988; 92: 145-159.
21. McNerney M, Pardi D, Pugh P, Nai Q, Margiotta J. Expression and channel properties of α-bungarotoxin-sensitive acetylcholine receptors on chick ciliary and choroid neurons. J Neurophysiol. 2000; 84: 1314-1329.
22. Murase KM, Randic T, Shirasaki T, Nakagawa T, Akaike N. Serotonin suppresses N-methyl-D-aspartate responses in acutely isolated spinal dorsal horn neurons of the rat. Brain Res. 1990; 525: 84-91.
23. Sigurdson WJ, Morris CE, Brezden BL, Gardner DR. Stretch activation of a K+ channel in molluscan heart cell. J Exp Biol. 1987; 127: 191-209.
24. Cuevas J, Adams DJ. Local anaesthetic blockade of neuronal nicotinic ACh receptor-channels in rat parasympathetic ganglion cells. Br J Pharmacol. 1994; 111: 663-672.
25. Adams DJ, Nutter TJ. Calcium permeability and modulation of nicotinic acetylcholine receptor-channels in rat parasympathetic neurons. J Physiol Paris. 1992; 86: 67-76.
26. Yawo H. Rectification of synaptic and acetylcholine currents in the mouse submandibular ganglion cells. J Physiol. 1989; 417: 307-322.
27. Sivilotti LG, McNeil DK, Lewis TM, Nassar MA, Schoepfer R, Colquhoun

D. Recombinant nicotinic receptors, expressed in Xenopus oocytes, do not resemble native rat sympathetic ganglion receptors in single-channel behaviour. J Physiol. 1997; 500: 123-138.

28. Weigand LA, Kwong K, Myers AC. The effects of nerve growth factor on nicotinic synaptic transmission in mouse airway parasympathetic neurons. Am J Respir Cell Mol Biol. 2015; 53: 443-449.

29. Crespi A, Plutino S, Sciaccaluga M, Righi M, Borgese N, Fucile S, et al. The fifth subunit in *α3β4* nicotinic receptor is more than an accessory subunit. FASEB J. 2018; 32: 4190-4202.

30. Krashia P, Moroni M, Broadbent S, Hofmann G, Kracun S, Beato M, et al. Human *α3β4* neuronal nicotinic receptors show different stoichiometry if they are expressed in xenopus oocytes or mammalian HEK293 cells. PLoS One. 2010; 5: e13611.

31. Grishin AA, Wang CA, Muttenthaler M, Alewood PF, Lewis RJ, Adams DJ. *α*-Conotoxin AuIB isomers exhibit distinct inhibitory mechanisms and differential sensitivity to stoichiometry of *α3β4* nicotinic acetylcholine receptors. J Bio Chem. 2010; 285: 22254-22263.

32. Yamaya H, Basaki Y, Togawa M, Kojima M, Kiniwa M, Matsuura N. Down-regulation of Th2 cell mediated murine peritoneal eosinophilia by antiallergic agents. Life Sci. 1995; 56: 1647-1654.

33. Mimura T, Shinozaki Y, Kawasaki H, Iwamura H. JTP-27536 [(+)-1,3-dihydroxy-2-hydroxymethylpropyl-2-ammonium-2-[(R)-3-cyclo-hexyl-1-phenylpropyl]-1,3-dioxo-2,3-dihydro-1H-isoindole-5-carboxylate monohydrate], a novel inhibitor of immunoglobulins and interleukin-5 with anti-inflammatory properties in mouse allergic dermatitis model. J Pharmacol Exp Ther. 2005; 314: 293-301.

34. Agrawal DK, Cheng G, Kim MJ, Kiniwa M. Interaction of suplatast tosilate (IPD) with chloride channels in human blood eosinophils: a potential mechanism underlying its anti-allergic and anti-asthmatic effects. Clin Exp Allergy. 2008; 38: 305-312.

35. Matsumoto S. Functional evidence of excitatory M1 receptors in the rabbit airway. J Pharmacol Exp Ther. 1997; 281: 531-539.

36. Bolser DC, DeGennaro FC, O'Reilly S, Hey JA, Chapman RW. Pharmacological studies of allergic cough in the guinea pig. Eur J Pharmacol. 1995; 277: 159-64.

37. Zhou JR, Shirasaki T, Soeda F, Yokomizo K, Takahama K. Direct Potentiation of Capsaicin Current by Histamine and Its Effect by Suplatast on Rat Trigeminal Ganglia Neurons. Pharmacol. 2018; 102: 37-41.

38. Matsuura N, Togawa M, Mori H, Nagai H, Koda A. The effect of suplatast tosilate on type allergic reactions. Jpn Pharmacol Ther. 1992; 20: 73-83.